Fourier Transform-Raman Spectroscopic Study of Natural Resins of Archaeological Interest

RACHEL H. BRODY,[1,2] HOWELL G. M. EDWARDS,[1] A. MARK POLLARD[2]

[1] Department of Chemical and Forensic Sciences, University of Bradford, Bradford, West Yorkshire BD7 1DP, United Kingdom

[2] Department of Archaeological Sciences, University of Bradford, Bradford, West Yorkshire BD7 1DP, United Kingdom

Received 25 July 2001; revised 1 October 2001; accepted 16 October 2001

ABSTRACT: Resins from several different genera are studied using Fourier transform (FT)-Raman spectroscopy. Tree resins can be broadly divided into those that contain diterpenoid components and those that contain triterpenoid components. The diterpenoid resins analyzed are from the genera *Pinus*, *Cedrus*, and *Agathis* (kauri resin) and the triterpenoid resins examined are samples from *Pistacia*, *Boswellia* (frankincense), and *Commiphora* (myrrh) genera. A protocol is developed to nondestructively distinguish diterpenoid and triterpenoid resins and to differentiate the genera within the two types. The effects of oxidation on the discrimination of the FT-Raman spectra are considered. © 2002 Wiley Periodicals, Inc. Biopolymers (Biospectroscopy) 67: 129–141, 2002

Keywords: Fourier transform-Raman spectroscopy; resins; diterpenoids; triterpenoids

INTRODUCTION

Tree resins have been used extensively throughout history because of a number of extremely useful properties including insolubility in water, glasslike characteristics, and adhesive properties.[1] Angiosperms and gymnosperms contain species that are resin producers. Tree resins are composed of terpene and terpenoid compounds, and diterpenoids (C_{20}) and triterpenoids (C_{30}) are the most common. Diterpenoids and triterpenoids have not been found together in a resin; thus, resins from each group have differing properties.[2] For example, the triterpenoid resins of genera such as *Pistacia* have been valued as varnishes on their own or blended with other resins such as dammar.[3] They yellow less and are more durable than diterpenoid resins such as those of the *Pinus* species.[2] Pine resins have been utilized by various cultures, including Native American tribes, for a number of functions such as waterproofing and sealing of baskets and as an adhesive to repair pottery.[1] Frankincense and myrrh, which are resins that contain triterpenoid components, are most often associated with the manufacture of incense; but they have also been used in several cultures for their medicinal properties. Myrrh is a mild disinfectant and has been used in embalming and as part of cosmetic preparations.[4] The use of natural resins has declined since the introduction of synthetic materials. However, natural resins are still used for certain purposes. For example, essential oils derived from natural resins are employed in the perfume industry and many res-

Correspondence to: R. H. Brody (R.H.Brody@bradford.ac.uk).

Biopolymers (Biospectroscopy), Vol. 67, 129–141 (2002)

Table I. Analyzed Resin Samples

Species	Location	Collection Period
Pistacia lentiscus (a)	Chios or Cyprus	Recent
Pistacia lentiscus (b)	Chios	Recent
Pistacia lentiscus[a] (c)	Chios	Before 1877
Pistacia terebinthus[a] (a)	Cyprus	Before 1885
Pistacia terebinthus[a] (b)	Possibly India	Before 1880
Pistacia mutica[a]	Possibly India	Before 1880
Pistacia khinjuk[a]	Possibly India	Before 1880
Pinus halepensis	Royal Botanical Gardens, Kew, Surrey, U.K.	Recent
Pinus pinea	Royal Botanical Gardens, Kew, Surrey, U.K.	Recent
Cedrus atlantica	Royal Botanical Gardens, Kew, Surrey, U.K.	1998
Cedrus libani	Unknown	Unknown
Boswellia (species unknown, frankincense)	Unknown	Unknown
Commiphora (species unknown, myrrh)	Unknown	Unknown
Agathis (species unknown, kauri resin)	Australia	Recent

All samples came from the collection of Dr. B. Stern at the University of Bradford.
[a] Donated originally by the Kew Economic Botany Collection (Royal Botanical Gardens, Kew, U.K.).

ins are used in alternative medicines; in the Ayurvedic system of medicine, *Boswellia serrata* resin is used as a cure for rheumatoid arthritis and gout.[5]

Fourier transform (FT)-Raman spectroscopy has potential as a nondestructive and noninvasive means of identifying both ancient and modern resin samples *in situ*. Various techniques have been applied to this end, the principal one being gas chromatography–mass spectrometry (GC–MS). The different components within the resins can be used as molecular markers for the determination of the biological source and to monitor the extent of degradation (i.e., the effects of processes such as oxidation and hydrolysis). However, techniques such as GC–MS require destruction of a small sample of material and cannot be carried out *in situ*. FT-Raman spectroscopy therefore has advantages for nondestructive resin analysis, particularly in the field of archaeological sciences.

Previous studies in our laboratory showed the potential for FT-Raman spectroscopy in the study of natural resins.[6–11] Much of this work concentrated on identifying archaeological resin samples. Spectroscopic differences were noted between resin samples without a full understanding of how chemical alteration brought about by processes such as oxidation might have on the spectra. This is the first comprehensive study of modern samples that is undertaken with consideration of the effects of processes such as oxidation.

MATERIALS AND METHODS

Samples

Resins from species within the genera *Pinus*, *Cedrus*, and *Pistacia* were analyzed along with samples of frankincense (genus *Boswellia*), myrrh (genus *Commiphora*), and kauri resin (genus *Agathis*) where the exact species was not known. Table I lists the analyzed samples with details of where and when they were collected, when known.

FT-Raman Spectroscopy

Raman spectra were obtained using a Bruker IFS66 instrument with a FRA106 Raman module attachment and Nd^{3+}/YAG near-IR excitation at 1064 nm. Spectra were recorded at 4 cm^{-1} resolution and 4000 scans accumulation. A nominal laser power of about 150 mW was used with a footprint of approximately 100 μm. Three replicate spectra were collected from each sample for comparison.

RESULTS AND DISCUSSION

Diterpenoid Resins

Resins from species of *Pinus* and *Cedrus* contain components with predominantly abietane skeletons and some components with pimarane skeletons. The pinyons of North America (e.g., *Pinus*

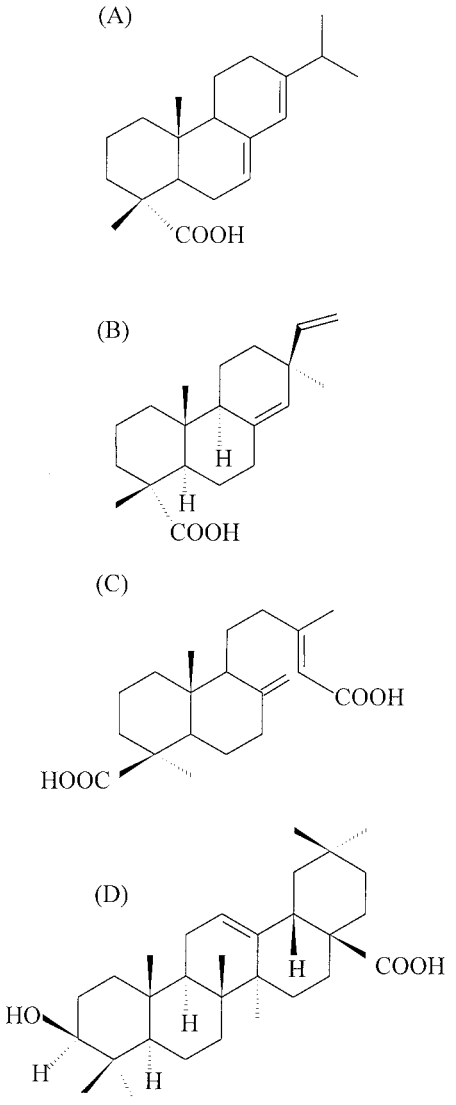

Figure 1. The structures of (A) abietic acid (13-isopropylpodocarpa-7,13-dien-15-oic acid), (B) pimaric acid [13(R)-podocarpa-8(14), 18-dien-15-oic acid], (C) agathic acid [labd-8(20), 13-dien-15, 18-dioic acid], and (D) oleanolic acid (3β-hydroxy-olean-12-en-28-oic acid).

monophylla) are the exception, containing mostly pimarane components with lesser concentrations of compounds with abietane skeletons. *Agathis* resins contain components based on the labdane skeleton. The structures of examples of compounds with each type of skeleton are shown in Figure 1. The University of Bradford GC–MS studies of some of the resin samples identified several key components.[12] Resin from *P. halepensis* was found to contain dehydroabietic acid (13-isopropylpodocarpa-8,11,13-trien-15-oic acid), 7-oxo-dehydroabietic acid, and abietic acid (13-isopropylpodocarpa-7,13-dien-15-oic acid). The *P. pinea* and *Cedrus libani* resins contain dehydroabietic acid and 7-oxo-dehydroabietic acid with pimaric [13(R)-podocarpa-8(14), 18-dien-15-oic acid] and sandaracopimaric [13(S)-podocarpa-8(14), 18-dien-15-oic acid] acids are also identified in the GC–MS trace of the former. This information about the resin samples was used to help assign the FT-Raman spectra. A sample of abietic acid was obtained from Sigma Chemicals Ltd., and the spectrum was used to aid assignment of the spectra collected from the resin samples.

The structure of abietic acid is shown in Figure 1(A). Stack plots of the spectra of the *P. pinea* resin, the *P. halepensis* resin, and abietic acid are shown in Figure 2 and Table II gives assignments for their vibrational modes. The strongest band in the spectra of the *P. pinea* and *P. halepensis* resins is that at approximately 2931 cm^{-1}, which is assigned to $\nu(CH_2)$ and $\nu(CH_3)$ (not shown). This complex feature is also seen in the spectrum of abietic acid and has a very similar profile in spectra of both the resins and abietic acid. Both *Pinus* resins have a shoulder at approximately 3053 cm^{-1} that is assigned to ν(CH) aromatic stretching. In the 1800–650 cm^{-1} wavenumber region the spectra of the diterpenoid resins show both inter- and intrasample variation. Three spectra were collected from each of the resin samples, and those from the *P. pinea* resin sample differ significantly. A stack plot in the 1800–650 cm^{-1} wavenumber region of the three spectra collected from the *P. pinea* resin is shown in Figure 3. (Spectrum b in Fig. 3 is the same as spectrum II in Fig. 2.) Spectrum a in Figure 3 collected from the *P. pinea* sample has broader band envelopes and a decrease in intensity or loss of some of the weaker features. Despite these differences, the main spectral features are still observed. This spectrum is therefore of an area of the sample that has been subject to a greater degree of degradation. The term degradation is used here to describe a combination of processes such as oxidation and hydrolysis that, in time, alter the chemical composition of natural resins.

The most dominant band in the spectrum of abietic acid is the strong, sharp band at 1649 cm^{-1} that is assigned to trans conjugated ν(C═C). The associated medium intensity feature at 1611 cm^{-1} is assigned to ν(C═C) of an aromatic ring. The sample of abietic acid is not 100% pure and it is possible that some dehydroabietic acid is present. There is only a very weak band at 1000 cm^{-1} because the aromatic ring in dehy-

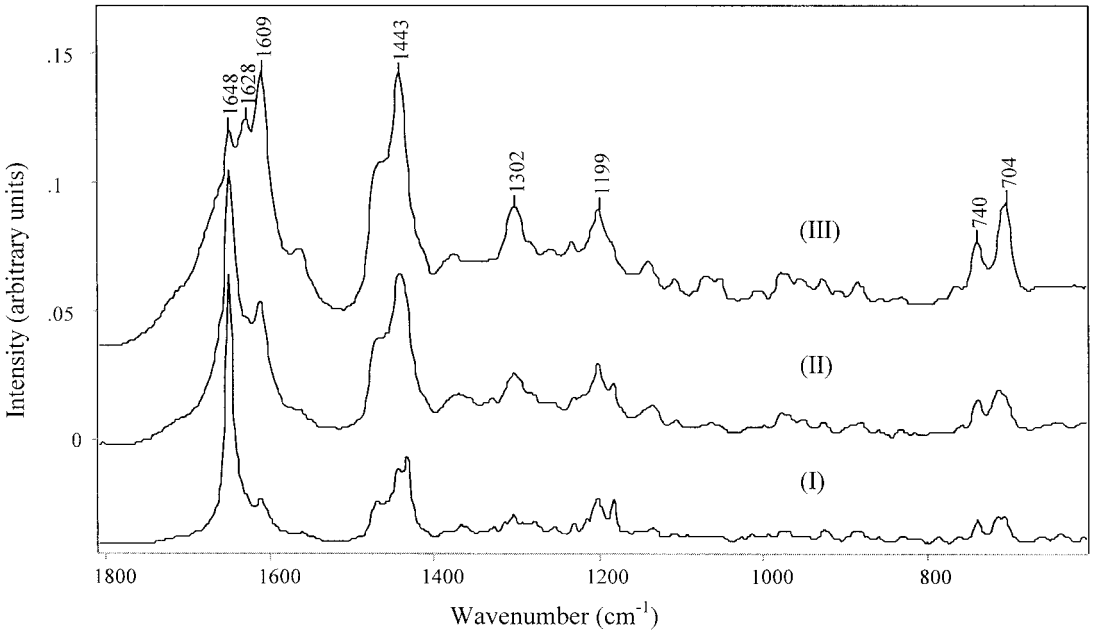

Figure 2. A stack plot of the FT-Raman spectra of abietic acid (spectrum I), *Pinus pinea* resin (spectrum II), and *Pinus halepensis* resin (spectrum III). (The spectra are normalized to the most intense band.)

droabietic acid is effectively trisubstituted. The intensity of the band at 1611 cm^{-1} is much increased relative to the band at 1649 cm^{-1} in the spectra of the resins. The *P. pinea* resin spectrum a in Figure 3 has similar intensities at 1649 and 1611 cm^{-1} while in the other two spectra of the same resin the band at 1649 cm^{-1} is more intense than that at 1611 cm^{-1}. A shoulder at 1631 cm^{-1} is seen in all three of the spectra collected from the *P. pinea* resin. In the spectra collected from the *P. halepensis* resin sample the band at 1611 cm^{-1} is more intense than that at 1649 cm^{-1}. A band can also be seen in all three *P. halepensis* resin spectra at 1629 cm^{-1}, which in one spectrum appears more intense than the band at 1649 cm^{-1}. The GC–MS results for the two *Pinus* resins showed that these two resin samples contained dehydroabietic acid and its 7-oxo derivative. Dehydroabietic acid is a product of oxidation and can be found in relatively fresh resins. The differences in the relative intensities of the bands at 1649 cm^{-1} (associated with abietic acid) and that at 1611 cm^{-1} (associated with dehydroabietic acid) between the spectra indicates different levels of degradation of the resin samples. The band profile between 1750 and 1550 cm^{-1} is much broader in the *P. halepensis* resin spectra compared with spectra b and c from the *P. pinea* resin sample in Figure 3, further suggesting the *P. halepensis* resin sample is more degraded. The band at 1629 cm^{-1}, which is assigned to ν(C═C) conjugated with a C═O, is also more intense in the *P. halepensis* resin spectra, suggesting an increase in the concentration of this moiety (i.e., the presence of compounds such as 7-oxodehydroabietic acid). The band profile between 1750 and 1550 cm^{-1} of spectrum a in Figure 3 collected from the *P. pinea* resin is very similar to that of *P. halepensis*, although the relative intensities of the bands at 1649 and 1611 cm^{-1} differ slightly. After undergoing further degradation, it is likely that the two resins will produce similar band profiles in the wavenumber range of 1750–1550 cm^{-1}, so the differences cannot be attributed to a difference in the resin-producing species.

The complex spectral feature centered on 1440 cm^{-1} in the spectra of the *Pinus* resins and abietic acid is assigned to CH_2 and CH_3 deformation modes. The number of these modes will increase as oxidation and hydrolysis cause different compounds to be produced. Three main bands at 1470, 1443, and 1433 cm^{-1} are seen in the spectrum of abietic acid and the latter is the most intense (Fig. 2). Again, the shape of this complex feature changes with the apparent associated change in the state of degradation of the sample. In all the spectra collected from the *P. pinea* and *P. halepensis* resin samples the most intense

Table II. Approximate Assignment of Vibrational Modes for FT-Raman Spectra of Abietic Acid and Diterpenoid Resins

Abietic Acid	*Pinus pinea*	*Pinus halepensis*	"Fake Frankincense"	*Cedrus atlantica*	*Cedrus libani*	Kauri Resin	Approx Assignment
3200 w, br					3202 vvw, br		ν(OH)
				3079 vvw		3081 w	ν(C═CH) olefinic
	3051 vw, sh	3054 w, sh			3052 w, sh		ν(CH) aromatic
3023 m, sh							Unsaturated ν(CH)
2979 w, sh	2979 m, sh	2979 w, sh	2981 mw, sh	2984 mw, sh	2980 mw, sh	2986 m, sh	$\nu(CH_2)$, $\nu(CH_3)$ symmetric
2952 m, sh	2951 m, sh	2951 w, sh	2951 ms, sh	2952 m, sh	2951 mw, sh		$\nu(CH_2)$, $\nu(CH_3)$
						2945 w, sh	$\nu(CH_2)$, $\nu(CH_3)$
2934 s	2931 vs	2932 vs	2931 vs	2924 vs	2932 vs	2931 vs	$\nu(CH_2)$, $\nu(CH_3)$
2899 s, sh		2905 w, sh	2905 m, sh	2905 mw, sh	2905 mw, sh		$\nu(CH_2)$, $\nu(CH_3)$
	2895 w, sh					2890 m, sh	$\nu(CH_2)$, $\nu(CH_3)$
2870 s, sh	2870 ms, sh	2872 ms, sh	2869 s	2870 m	2871 m	2869 m, sh	$\nu(CH_2)$, $\nu(CH_3)$
				2847 mw, sh		2848 m, sh	$\nu(CH_2)$, $\nu(CH_3)$
2838 w, sh			2835 mw, sh	2835 w, sh			$\nu(CH_2)$, $\nu(CH_3)$
				1727 vw, br			
		1709 w, sh	1708 vw, br		1716 w, sh	1716 mw, sh	ν(C═O)
	1665 w, sh	1664 w, sh		1667 vw, sh	1662 m		
1649 vs	1649 s	1649 ms	1651 vs	1649 s	1651 mw, sh		ν(C═C) trans conjugated
						1646 s	ν(C═C) nonconjugated
	1631 m, sh	1629 ms			1636 mw		ν(C═C) conjugated with C═O
1611 m	1612 ms	1610 s	1611 ms	1611 m	1611 ms	1611 w, sh	ν(C═C) aromatic
1562 w	1563 w	1563 mw	1562 w, sh		1564 w		
1470 ms, sh	1469 m, sh	1469 m, sh	1471 m, sh	1470 m, sh	1470 m	1469 mw, sh	$\delta(CH_2)$, $\delta(CH_3)$
			1458 m, sh				
						1449 ms	
1443 ms	1442 ms	1443 ms	1442 ms	1439 ms, br	1443 s	1439 ms	$\delta(CH_2)$, $\delta(CH_3)$ scissors
1433 ms	1434 m, sh		1432 ms				$\delta(CH_2)$, $\delta(CH_3)$
		1415 w, sh		1412 w, sh	1416 w, sh	1410 mw	
	1382 w, sh		1384 mw, sh	1383 vw, sh		1385 vw, sh	
1368 mw	1372 mw	1376 w	1372 m	1373 mw	1377 vw	1373 mw	$\delta(CH_2)$, $\delta(CH_3)$
	1358 w	1355 vw	1360 mw, sh	1356 w, br		1358 mw	
1328 vw	1328 w	1332 vw, sh	1329 mw	1329 mw		1329 w	$\delta(CH_2)$, $\delta(CH_3)$
1304 mw	1302 m	1303 m	1303 m	1304 m, br	1303 m	1306 mw	$\delta(CH_2)$, $\delta(CH_3)$ twisting
	1284 w, sh	1281 w, sh	1282 m	1285 w, sh			
1279 mw	1278 w, sh						
						1245 mw	
1230 w	1229 w	1233 w		1232 mw	1233 w		
1215 w, sh	1215 w, sh		1217 mw, sh	1218 mw		1221 w, sh	
1201 m	1201 m	1200 m	1201 m	1201 m	1200 m	1203 w, sh	δ(CCH)
						1198 m, br	δ(CCH)
1182 m	1182 mw	1184 mw, sh	1184 m	1183 mw	1185 w, sh	1184 mw, sh	ν(CC) ring breathing
1134 mw	1134 mw	1139 mw	1133 mw	1139 mw	1140 mw	1136 mw	ν(CC) ring breathing
1109 w	1105 vw	1107 vw	1100	1105 w	1106 mw	1101 mw	
				1083 mw		1084 mw	
1067 w		1069 vw	1069 w		1070 mw		ν(COH)
1059 w	1062 vw			1061 w, sh		1062 mw	ν(COH)
1000 vw	1000 vw	1002 vw	1001 w	1000 mw	1001 vw		ν(CC) aromatic
978 mw	977 mw	978 mw	978 mw	978 w, sh	979 mw, br	981 w, sh	$\rho(CH_2)$, $\rho(CH_3)$
971 mw	970 w, sh	972 w, sh	968 mw	970 w		972 mw	$\rho(CH_2)$, $\rho(CH_3)$
951 w	951 w	955 w	949 mw	952 mw	952 w, br	950 w, sh	
				945 mw, sh			
						936 mw	
927 mw	927 mw	928 mw	925 mw	928 mw	928 mw	928 mw	
		907 w		905 mw	907 vw	906 w	
890 mw	892 mw, sh						
883 mw	882 mw	885 mw	883 mw	885 mw	884 w	883 mw, br	
				841 mw	838 vw	842 mw	
788 w				770 mw		770 mw	
762 w							
740 m	740 m	740 m	742 mw	744 mw	740 m	741 m, br	ν(CC) isolated

Table II. *Continued*

Abietic Acid	*Pinus pinea*	*Pinus halepensis*	"Fake Frankincense"	*Cedrus atlantica*	*Cedrus libani*	Kauri Resin	Approx Assignment
716 m	715 m		715 m	711 m		717 mw	ν(CC) isolated
708 m	709 vw, sh	706 m	708 w, sh	704 m, sh	707 m		ν(CC) isolated
568 vw			569 w	563 mw		565 mw	
548 mw	550 mw	552 mw	557 mw	551 mw	554 w	553 w, sh	δ(CCO)
534 vvw	534 mw	532 mw	537 w	535 mw		540 vw, sh	
				480 mw		481 w	
475 mw, sh	474 mw, sh	472 vw, sh	474 mw				δ(CCC)
		464 mw, sh		462 mw	463 mw		
455 m	454 mw	455 mw	454 m	453 vw, sh		450 mw, br	δ(CCO)
428 w	428 vw	429 vvw	429 mw	426 w		427 vw, br	
374 m	372 mw	370 mw	371 mw	368 mw	368 mw	366 mw, br	δ(CCC)
305 vw	307 vw	306 vw	304 vw, sh	307 mw	302 mw, br	304 mw, br	
226 m	226 m	226 m	225 m				$\tau(CH_3)$
			215 mw, sh	210 mw, br	216 mw, br		

band is observed at 1442 cm^{-1}, and there is little change occurring to the shape of the band at 1470 cm^{-1}. In spectra b and c in Figure 3 collected from the *P. pinea* resin sample a shoulder is seen at 1434 cm^{-1}, which can be associated with the band seen at 1433 cm^{-1} in the spectrum of abietic acid. This band appears to become so weak in comparison with that at 1442 cm^{-1} that it does not appear as a shoulder in the *P. pinea* spectrum a or the spectra of the *P. halepensis* resin.

In the wavenumber region of 800–680 cm^{-1} (Fig. 2) there are five bands of weak intensity in the spectrum of abietic acid at 788, 762, 740, 715, and 708 cm^{-1}; the latter two form a doublet and are assigned to isolated ν(CC). The doublet is not evident in the spectra of the two *Pinus* resins with a broad band being centered at 715 cm^{-1} in spectra b and c of Figure 3 from the *P. pinea* resin and at 706 cm^{-1} for the *P. halepensis* resin spectra and spectrum a of Figure 3 from the *P. pinea* resin sample. The *P. pinea* spectra b and c have a weak shoulder at 709 cm^{-1}, indicating that the change in the profile of this feature is more complex than simply a change in the band position. The bands at 762 and 740 cm^{-1} decrease in intensity relative to the band at 715/709 cm^{-1} when comparing the *Pinus* resin spectra with the spectrum of abietic acid, the least intense being in the *P. halepensis*

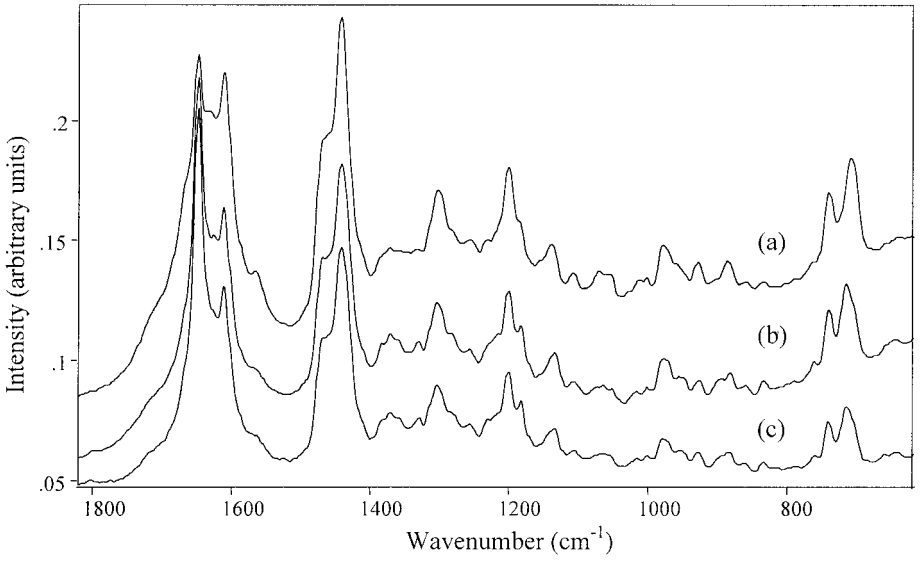

Figure 3. A stack plot of three FT-Raman spectra collected from the *Pinus pinea* resin sample. (The spectra are normalized to the most intense band.)

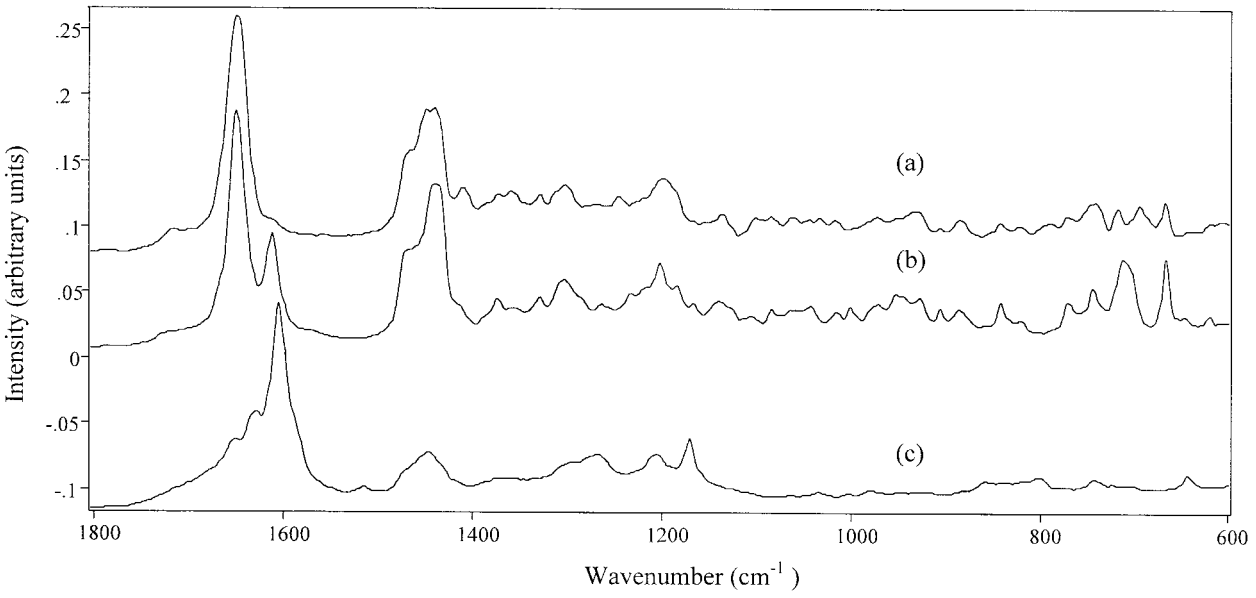

Figure 4. A stack plot of the FT-Raman spectra of kauri resin (genus *Agathis*, spectrum a), *Cedrus atlantica* resin (spectrum b), and *Pinus monophylla* resin (spectrum c).

resin. The band at 788 cm^{-1} is only found as a very weak band in the *Pinus* resin spectra.

Differences in the relative band intensities and band broadening between the *Pinus* resin and abietic acid spectra are also seen in the wavenumber regions not discussed. Both *Pinus* resins produce spectra that are closely related to that of abietic acid. Although the *Pinus* resins contain other components, the predominant structures are clearly all similar to the skeletal structure of abietic acid. The only band that was noted in the spectra of the *Pinus* resins that was not seen in the spectrum of abietic acid is that at approximately 1629 cm^{-1}, which is assignable to ν(C═C) conjugated with C═O. The differences between the spectra collected from the two *Pinus* resins, as well as the differences between the three spectra from the *P. pinea* resin sample, are attributable to the affects of oxidation and hydrolysis rather than species.

Table II contains assignments for bands in the spectra of the two samples of resin from the genus *Cedrus*. The spectra collected from the *C. libani* resin (not shown) were very similar to those of the *P. halepensis* resin (Fig. 2). The relative intensities of the main spectral features were the same in both (1443 > 1611 > 1302 > 1200 cm^{-1}). The *C. atlantica* resin spectra (Fig. 4, spectrum b) were most similar to the *P. pinea* spectra (Fig. 3, spectra b and c). The *C. atlantica* resin produces spectra with better resolved and sharper bands than the *C. libani* or *Pinus* resins. This indicates that the *C. atlantica* resin sample is not as degraded as the *C. libani* or *Pinus* resins. It is thought that with time this resin will produce spectra that, like those of *C. libani*, cannot be distinguished from those of *Pinus* resins.

The FT-Raman spectra of other *Pinus* resins that we reported previously include *P. monophylla* resin, which is a pinyon native to the southwestern region of the United States, and *P. keysia* resin from Vietnam.[7,9] The spectra of the *P. keysia* resin were compared with those of the two pine resins analyzed during this research and were found to be very similar.[9] The spectra of the *P. monophylla* resin (Fig. 4, spectrum c) were also compared and were found to differ significantly from those of the *Pinus* and *Cedrus* resins. The most noticeable difference between the FT-Raman spectra is the position of the most intense band. In each of the spectra of the *Pinus* and *Cedrus* resins the band at approximately 2930 cm^{-1} that is assigned to ν(CH) modes is the most intense, but in *P. monophylla* spectra the most intense band is at 1605 cm^{-1} that is assigned to isolated ν(C═C). The band at 1442 cm^{-1}, which is assigned to $\delta(CH_2)$ and $\delta(CH_3)$ modes, is also much less intense in the spectra of *P. monophylla* resin than in the spectra of the other pine and cedar resins. The difference in the intensity of bands assigned to ν(CH) and δ(CH) modes relates

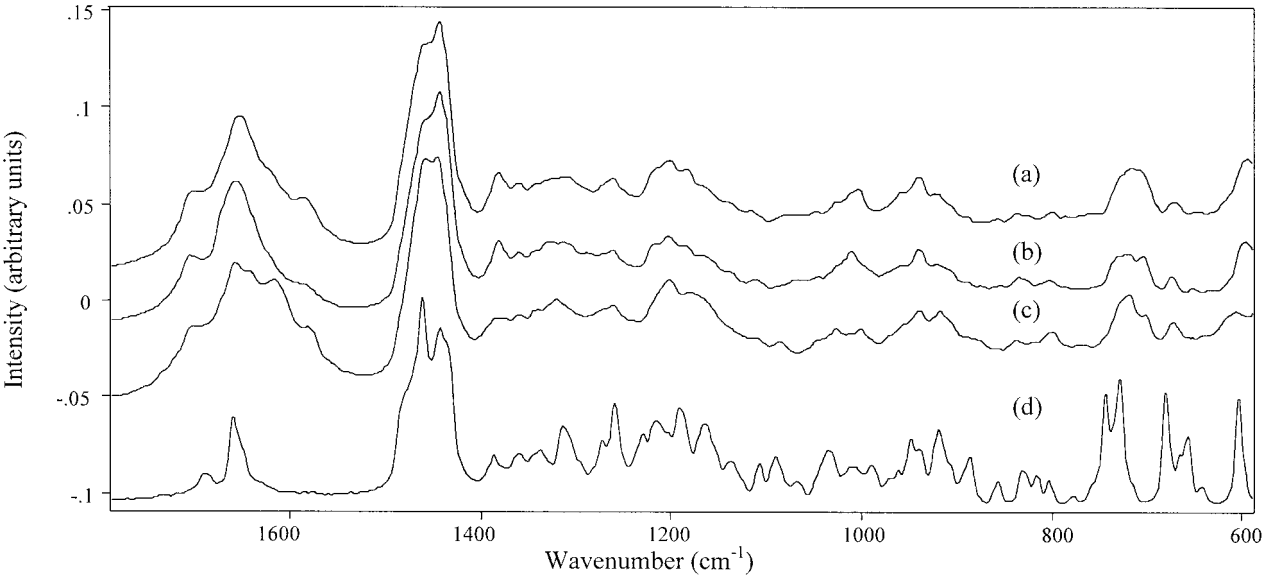

Figure 5. A stack plot of the FT-Raman spectra of *Pistacia terebinthus* resin (spectrum a), *Pistacia lentiscus* resin (spectrum b), *Pistacia mutica* resin (spectrum c), and oleanolic acid resin (spectrum d).

to the abietane skeleton having an isopropyl group that is not present in the pimarane skeleton. (This difference between abietic acid and pimaric acid can be seen in Fig. 1.)

The spectra collected from the kauri resin, species *Agathis*, are quite different than the spectra of abietic acid and *Pinus* and *Cedrus* resins (Fig. 4, spectrum a). The FT-Raman spectra of the kauri resin appear to be easily distinguished due to the presence and absence of certain bands. A weak feature is seen at 3081 cm^{-1} that is assigned to the ν(CH) vibration of the exocyclic methylene group found in many compounds with a labdane skeleton [e.g., agathic acid in Fig. 1(C)]. The prominent band at 1611 cm^{-1} seen in the *Pinus* and *Cedrus* resin spectra is absent with bands present at 1198, 936, and 181 cm^{-1}. The kauri resin spectrum is the least similar to that of abietic acid out of the three diterpenoid resins considered, which is to be expected because the diterpenoids in the kauri resin are thought to have a labdane skeleton. If abietic acid is present, it is only a minor constituent and little or no dehydroabietic acid would appear to have been produced.

Triterpenoid Resins

The GC–MS studies of one of the *Pistacia* resins identified some of the key components. The triterpenoids moronic acid (3-oxo-olean-18-en-28-oic acid), oleanonic acid (3-oxo-olean-12-en-28-oic acid), isomasticadienoic acid (3-oxo-13α,14β,17βH, 20αH-lanosta-8,24-dien-26-oic acid), and masticadienoic acid (3-oxo-13α,14β,17βH,20αH-lanosta-7,24-dien-26-oic acid) were the four most abundant compounds identified in *Pistacia lentiscus* resin. Oleanolic acid (3β-hydroxy-olean-12-en-28-oic acid) was obtained (Sigma) so that the spectra could again be used to aid assignment of the spectra collected from the resin samples.

Oleanolic acid is a triterpenoid with the same skeletal structure as several of the components identified in *Pistacia* resins. The structure of oleanolic acid is shown in Figure 1(D). The FT-Raman spectrum of oleanolic acid and spectra from *Pistacia terebinthus*, *Pistacia lentiscus,* and *Pistacia mutica* resins are shown in Figure 5 and the vibrational modes are detailed in Table III. The spectrum of oleanolic acid is highly complex because of its pentacyclic structure and it is thus difficult to assign all the bands unambiguously. However, regions of the spectrum are known to be associated with particular modes. The 3000–2600 cm^{-1} wavenumber region contains bands assigned to the ν(CH) of CH_2 and CH_3 symmetric and asymmetric stretches. The associated deformation modes [$\delta(CH_2)$ and $\delta(CH_3)$] are found in the 1490–1300 cm^{-1} wavenumber region with methyl group rocking vibrations at approximately 948 cm^{-1} and methyl torsions at approximately

Table III. Approximate Assignment of Vibrational Modes for FT-Raman Spectra of Oleanoic Acid and Resins from Various Species of *Pistacia* Trees

Oleanolic Acid	*Pistacia terebinthus*		*Pistacia mutica*	*Pistacia khinjuk*	*Pistacia lentiscus*			Approx Assignment
	a	b			a	b	c	
			3171 vw, br	3165 vvw, br				
3003 w, sh								$\nu(CH_2)$, $\nu(CH_3)$
2978 w, sh								$\nu(CH_2)$, $\nu(CH_3)$
2967 w, sh	2969 mw, sh	2968 m, sh	2969 m, sh	2968 mw, sh	2966 mw, sh	2964 mw, sh	2963 m, sh	$\nu(CH_2)$, $\nu(CH_3)$
2941 w, sh					2945 mw, sh	2945 mw, sh	2945 mw, sh	$\nu(CH_2)$, $\nu(CH_3)$
2933 vs	2930 vs	2931 vs	2932 vs	2930 vs	2927 vs	2930 vs	2930 vs	$\nu(CH_2)$, $\nu(CH_3)$
2912 mw, sh					2911 mw, sh	2914 mw, sh		$\nu(CH_2)$, $\nu(CH_3)$
2896 mw, sh								$\nu(CH_2)$, $\nu(CH_3)$
2880 mw, sh								$\nu(CH_2)$, $\nu(CH_3)$
	2873 m, sh	2874 m, sh	2869 m	2873 m, sh	2873 m, sh	2873 m, sh	2873 mw, sh	$\nu(CH_2)$, $\nu(CH_3)$
2865 mw								
	1701 m, sh	1705 mw, sh	1704 m, sh	1704 mw, sh	1705 m	1705 m	1705 m	
1689 mw								
				1668 m, sh				ν(C═C)
1659 m	1653 ms	1653 mw	1657 m	1654 ms	1660 ms	1660 ms	1658 ms, br	ν(C═C)
1649 mw, sh					1649 m, sh	1649 mw, sh		ν(C═C)
1629 vw, sh	1623 mw, sh	1620 w, sh	1616 m	1619 m, sh				
	1587 m	1584 w, sh	1581 mw	1584 mw, sh			1585 mw	
1481 m, sh	1478 w, sh				1479 mw, sh	1479 mw, sh	1478 w, sh	$\delta(CH_2)$, $\delta(CH_3)$
1461 s	1462 m, sh	1459 m, sh	1458 ms	1460 m, sh	1460 m, sh	1462 m, sh	1460 m, sh	$\delta(CH_2)$, $\delta(CH_3)$
1443 ms	1443 ms	1444 m	1445 ms	1443 s	1441 s	1442 s	1442 s	$\delta(CH_2)$, $\delta(CH_3)$
1433 m, sh								$\delta(CH_2)$, $\delta(CH_3)$
1387 m			1385 mw					$\delta(CH_2)$, $\delta(CH_3)$
1379 m	1381 mw	1379 mw	1377 mw	1379 m	1380 m	1381 m	1381 m	$\delta(CH_2)$, $\delta(CH_3)$
1360 mw	1360 w	1361 vw	1360 mw	1360 w	1360 mw	1360 w	1359 w	$\delta(CH_2)$, $\delta(CH_3)$
1338 mw	1342 vw, sh		1341 mw	1341 vvw	1344 vw, sh	1344 w, sh	1343 vw, sh	$\delta(CH_2)$, $\delta(CH_3)$
	1329 vw, sh	1330 w		1329 w	1329 m	1329 m	1328 m	$\delta(CH_2)$, $\delta(CH_3)$
			1320 m	1317 vvw				$\delta(CH_2)$, $\delta(CH_3)$
1313 m								$\delta(CH_2)$, $\delta(CH_3)$
1306 mw, sh	1306 mw, br	1304 w		1305 vvw	1309 mw	1306 mw	1307 m	$\delta(CH_2)$, $\delta(CH_3)$
					1285 mw	1284 vw	1286 w	
1272 mw			1272 w				1274 vw	δ(CCH)
1259 m	1261 mw	1262 w	1262 mw	1261 mw	1261 mw	1262 w	1261 w	δ(CCH)
1230 mw								δ(CCH)
1217 mw	1216 mw, sh	1217 w	1213 w, sh	1215 mw, sh	1217 mw	1217 mw	1216 w	δ(CCH)
1203 vw, sh	1201 m	1203 w	1203 m	1202 m	1202 m	1202 m	1202 m, br	δ(CCH)
1191 m								ν(CC) ring breathing
	1183 mw	1183 w	1180 mw	1184 w	1184 mw	1184 mw	1184 w, sh	
1164 m, br	1164 mw, sh			1166 w	1163 mw	1165 w	1165 w, sh	ν(CC) ring breathing
		1085 mw	1086 w	1085 mw	1084 w	1083 vw	1085 w	
1034 mw								ν(C═O)
	1026 w		1028 mw	1025 vw	1027 mw, sh	1027 w, sh	1026 mw, sh	
1012 w, sh	1011 mw, sh	1010 w	1011 vw, sh	1010 mw, br	1010 m	1010 m	1010 m	
1007 w	1003 m, br		1001 mw		997 mw, sh	995 w, sh	1000 w, sh	δ(CC) aromatic ring breathing
961 vw	958 mw, sh		958 mw, sh	952 mw, sh	957 mw, sh	957 vw	958 w	
948 m								$\rho(CH_3)$
939 mw	939 m	940 mw	939 m	941 m	938 m	938 m	938 m	$\rho(CH_3)$
919 m	920 w	921 vw	917 m	921 w, sh	919 mw		919 w, br	$\rho(CH_3)$
743 ms			745 w, sh					ν(CC) ring
728 ms	729 mw, sh			727 mw, sh	729 m	730 mw, sh	730 m, sh	ν(CC) ring
713 vw, sh	715 m, br		721 m	716 m, sh	718 m, sh	718 m	718 m	
	707 mw, sh	710 w		706 m				
			702 mw		702 m	702 mw	703 m	
680 ms								
	672 w		672 mw		673 m		673 mw	
657 m								

Table III. *Continued*

Oleanolic Acid	*Pistacia terebinthus* a	*Pistacia terebinthus* b	*Pistacia mutica*	*Pistacia khinjuk*	*Pistacia lentiscus* a	*Pistacia lentiscus* b	*Pistacia lentiscus* c	Approx Assignment
603 ms			605 w			599 mw, sh		
	594 m	597 vw		597 mw, br	594 m	593 m	594 m	
	581 mw, sh		581 w		581 m, sh	582 m, sh	582 m, sh	
562 ms	561 w	559 w	557 vw	563 mw	560 mw	560 w		
531 m	529 m		532 mw	530 w	529 mw	529 mw, br	529 mw	
473 mw, br			471 w, sh			476 w, sh		δ(CCC)
	464 mw	462 vvw	463 mw	464 mw	462 mw	463 mw	461 mw	
446 mw			450 vw, sh		448 mw, sh	448 w, sh	449 w, sh	δ(CCO)
408 mw, br	411 mw		412 mw	409 w, sh	411 mw, sh	411 mw	410 mw	
391 vw			389 mw, br	391 w, br	396 mw, sh	395 w, sh	399 w, sh	
262 mw	259 vvw		259 vw	256 vw		262 w, br	262 vw	$\tau(CH_3)$

262 cm^{-1}. Ring breathing modes [ν(CC)] are seen in the 1200–1100 cm^{-1} wavenumber region with further ν(CC) ring vibrations between 750 and 700 cm^{-1} and ring deformations [δ(CCC)] at approximately 473 cm^{-1}. Medium to weak intensity features are seen at 1034 and 446 cm^{-1} and these are assigned to ν(C—O) and δ(CCO), respectively.

The analysis of the spectra collected from the *Pistacia* resins is more difficult than that of the diterpenoid resins. The spectrum of oleanolic acid cannot be easily related to the spectra of the *Pistacia* resins. Differences are seen between the spectra of the four *Pistacia* resins, but these differences cannot be easily identified as being due to either species or degradation. Because the changes seen between the *Pinus* and *Cedrus* resins appear to be related to degradation rather than species or genera, it is likely that this is also the case with the *Pistacia* resins.

Frankincense contains a range of triterpenoid components including α- and β-boswellic acids (3α-hydroxy-olean-12-en-24-oic acid and 3α-hydroxy-urs-12-en-24-oic acid, respectively). Oleanolic acid has a very similar structure to both α- and β-boswellic acids, differing principally in the position of the carboxylic acid group. However, the bands seen in the frankincense spectra in

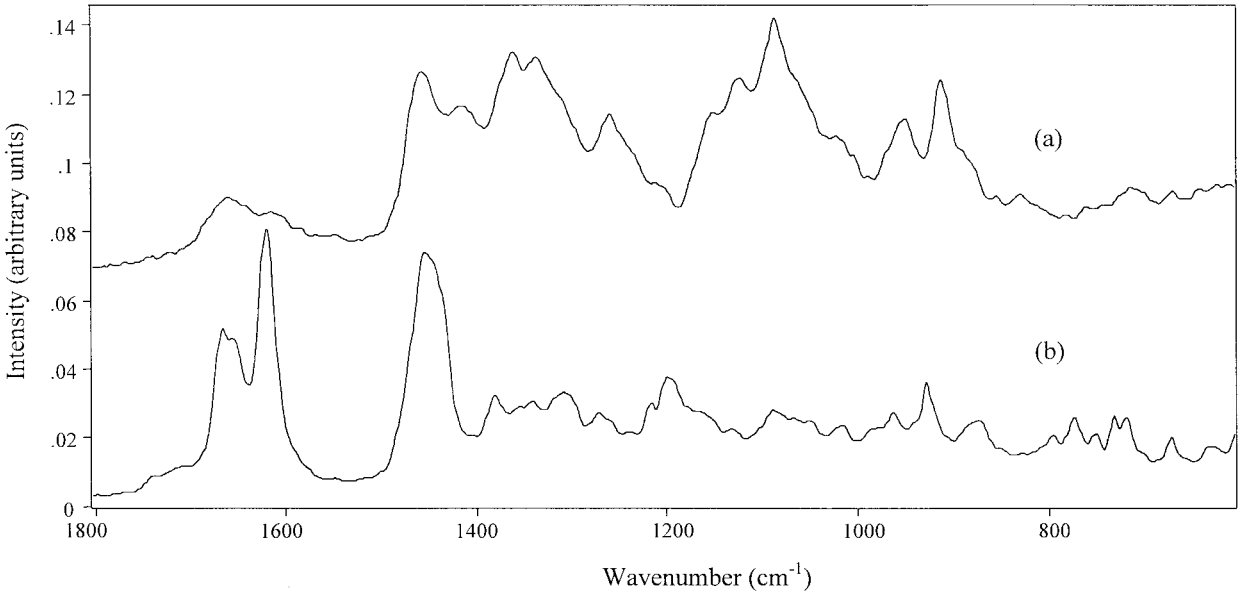

Figure 6. A stack plot of the FT-Raman spectra of myrrh (genus *Commiphora*, spectrum a) and frankincense (genus *Boswellia*, spectrum b).

Table IV. Approximate Assignment of Vibrational Modes for FT-Raman Spectra of Frankincense and Myrrh

Frankincense	Frankincense	Frankincense	Myrrh Yellow	Myrrh Black	Approx. Assignment
			3220 w, br	3214 vw, br	ν(NH) symmetric
			3063 vw		ν(C═CH)
2971 mw, sh	2971 mw, sh	2971 mw, sh	2980 vw, sh		$\nu(CH_2)$ symmetric
			2938 vs		$\nu(CH_3)$ asymmetric
2930 vs	2930 vs	2930 vs			$\nu(CH_3)$ asymmetric
				2921 vs	$\nu(CH_2)$
2912 w, sh	2912 w, sh	2912 w, sh			$\nu(C{=}CH_2)$
			2904 m, sh		
2874 m, sh	2874 m, sh	2874 m, sh			$\nu(CH_2)$ symmetric
2851 mw, sh	2851 mw, sh	2851 mw, sh	2848 w, sh	2848 m, sh	
				2800 w, sh	
2724 vw	2724 vw	2724 vw			$\nu(CHBCH_2{=}CH_2)$ backbone
1666 ms	1665 ms	1667 ms	1663 m	1664 m	ν(C═C) trans configuration
1656 mw, sh	1653 m, sh	1657 m, sh			ν(C═C) cis configuration
				1646 m	$\nu(CH{=}CH_2)$
1621 ms	1621 ms	1621 s			ν(C═C) isolated
			1613 mw		ν(C═C) isolated
				1593 ms	
				1563 ms	ν(C═O)
1455 ms	1455 ms	1455 ms	1457 ms	1450 ms, br	$\delta(CH_2)$ scissors
1445 m, sh	1445 m, sh	1445 m, sh	1446 vw, sh		$\delta(CH_2)$ scissors
			1415 m	1417 m	$\delta(CH_2)$
1380 m	1382 m	1380 m		1377 m	$\delta(CH_2)$
1357 w	1357 mw	1355 w	1361 ms	1362 w	$\delta(CH_2)$
1342 mw	1341 mw	1342 mw		1345 mw	$\delta(CH_2)$, δ(COH) wagging
			1337 ms	1337 w	$\delta(CH_2)$, δ(COH) wagging
1318 m, sh	1318 m	1318 m, sh	1315 mw, sh	1313 mw, sh	$\delta(CH_2)$, δ(COH)
1307 m	1307 m	1309 m			$\delta(CH_2)$ twisting
1301 mw, sh	1301 m	1301 m, sh			
1271 vw	1271 w	1272 mw			$\delta(CH_2)$
1259 vw	1259 vw	1259 w, sh	1260 m	1258 mw	δ(COH)
1216 mw	1216 mw	1216 mw	1212 vw		δ(COH)
1202 m	1201 m	1200 m		1206 vvw	δ(COH), δ(CCH)
	1193 w, sh	1193 m, sh			
		1178 mw, sh			
1175 mw	1175 w, sh				
1166 w, sh	1166 mw	1166 w			ν(C═O)
			1152 mw	1158 w	ν(CC) ring breathing
1126 w	1128 w		1124 m	1120 mw	ν(COC) symmetric
1093 vw, sh	1093 mw, sh			1096 w, sh	
		1089 m	1087 ms	1087 m	ν(CO)
1081 m	1081 m	1081 m, sh			ν(CO)
1067 vw, sh	1066 mw	1067 mw	1065 vw, sh		ν(CO)
1052 mw	1051 mw	1051 mw	1052 vw, sh		ν(CO)
1017 mw	1017 mw	1017 mw	1020 vw	1021 vw	ν(CO) in plane deformation
962 m	962 m	962 m	967 vw, sh	966 w, sh	$\rho(CH_2)$
			950 m	953 m	
	927 m	927 ms			$\rho(CH_3)$
922 mw	920 mw, sh			919 w, sh	$\rho(CH_3)$
			912 ms	913 m	$\rho(CH_3)$
875 mw	876 mw	873 w			$\rho(CH_2)$
772 m	772 m	772 m			$\delta(CH_2)$ rock
753 w	752 mw	750 mw			ν(CC) ring
				742 m	ν(CC) ring
731 mw	731 mw	731 m		729 mw, sh	$\delta(CH_2)$ rock

Table IV. *Continued*

Frankincense	Frankincense	Frankincense	Myrrh Yellow	Myrrh Black	Approx. Assignment
719 w, sh	719 mw, sh	718 m	713 w		ν(CC)
700 vvw	700 vvw	700 vvw		701 m, sharp	ν(CC) ring in plane twisting
671 mw	671 mw	671 mw	670 w		ν(CC)
				613 mw	
601 w	601 w, sh	601 w, sh		599 mw	δ(CC) ring deformation
590 w		590 w		588 mw	δ(CCO)
	585 mw				
558 mw	558 mw	558 mw	552 w		
545 w	545 w	545 w		547 m, sharp	δ(COC) glycosidic link
528 mw	528 mw	528 mw		522 mw	δ(COC) glycosidic link
492 mw	492 mw	492 mw		491 mw	δ(COC) glycosidic link
473 mw	473 mw	473 mw	474 mw, sh	472 w	δ(CCC)
465 w, sh	465 mw, sh	465 w, sh	462 mw, sh		δ(CCO) ring deformation
449 w	447 w	447 w	444 m	447 m	δ(CCO) ring deformation
			351 m	351 m	δ(CCC) ring
305 vvw	305 vw	305 vw		300 m	

Figure 6 cannot be easily related to those seen in the spectra of oleanolic acid. (An assignment table for frankincense and myrrh is provided in Table IV.) A proportion of frankincense (ca. 5–30%) is a gum made up of various polysaccharides. Although only seen as weak intensity bands, bands associated with the glycosidic linkage in polysaccharides can be identified in the spectra of frankincense. The bands at approximately 1126 and 1093 cm^{-1} are assigned to the ν(COC) of the respective symmetric and asymmetric glycosidic linkage. The bands at 545, 528, and 492 cm^{-1} are assigned to the δ(COC) of the glycosidic link. The polysaccharides may also contribute to the $\delta(CH_2)$ and $\rho(CH_2)$ modes seen at around 1450 and 950 cm^{-1}.

Myrrh is also a gum resin, but it has a much higher gum content: myrrh contains around 30–60% water-soluble gum while frankincense contains only 5–30%. The resin component is known to consist of triterpenoid components and the gum component of proteoglycans with dominating amounts of polymers rich in uronic acid.[13] As can be seen in Figure 6, the spectra of myrrh are very different than those of any of the other resins examined. Myrrh cannot be mistaken for any other resin because it has a high enough proportion of gum to make its spectra unlike those of any of the resins examined. However, the spectra of natural gums previously reported in the literature[11] are quite similar.

Distinguishing FT-Raman Spectra of Diterpenoid and Triterpenoid Resins

Because the spectra of diterpenoid and triterpenoid resins contain many similar bands, an assessment was made of which bands could be used to distinguish the spectra of any diterpenoid resin from those of any triterpenoid resin, regardless of the state of degradation. The relative intensities of the bands were found to be altered significantly with the state of degradation, so they are not generally useful for discrimination. Bands were also noted that can be used to distinguish spectra collected from the various diterpenoid resins from each other and the same was done for the triterpenoid resins. The resulting protocol is shown in Figure 7. Myrrh is not included because its spectra are so easily distinguished from those of the diterpenoid and triterpenoid resins. The protocol tries to account for the fact that spectral variations occur that are due to processes such as oxidation and hydrolysis. However, the effects of degradation will eventually result in these spectral differences becoming less easy to identify. It is unlikely that severely oxidized or hydrolyzed samples will provide clear enough spectra for identification purposes. Successful identification is possible on all modern resin samples as long as the effects of degradation are borne in mind. Well-preserved ancient tree resin specimens from whom good quality spectra can be collected can also be identified using this protocol.

(1) Determine whether the spectrum is of a diterpenoid or triterpenoid resin

- Bands at 1303, 977 and 740 cm^{-1} = diterpenoid
- Bands at 1380 and 530 cm^{-1} = triterpenoid

(2) Diterpenoids

- Medium to strong intensity bands at 1630 and 1611 cm^{-1} and a weak band at 3050 cm^{-1} suggest the presence of dehydroabietic and its 7-oxo derivative = resins based on abietane compounds e.g. European *Pinus* resins
- Bands at 3080, 1196 and 183 cm^{-1} = *Agathis* (kauri) resins (and probably other resins containing labdane compounds)
- Medium to strong intensity bands at 3062 and 1605 cm^{-1} along with bands at 1270 and 1170 cm^{-1} = resins based on pimarane compounds e.g. those of pinyon pines *i.e. Pinus monophylla* resin

(3) Triterpenoids

- Band or shoulder at 1705 cm^{-1}, a shoulder at 1183 cm^{-1} and bands at 939, 597 and 410 cm^{-1} = *Pistacia* resins

Bands at 962, 875, 492 cm^{-1} = frankincense

Figure 7. The protocol for the identification of a tree resin from its FT-Raman spectrum.

CONCLUSIONS

FT-Raman spectroscopy was shown to be a useful tool in the nondestructive discrimination of various tree resins. The genera studied are among the most common ones found in archaeological contexts. FT-Raman spectroscopy can now be considered for the nondestructive analysis of archaeological resin finds, particularly for *in situ* studies. Successful identification was made of archaeological resin samples in our laboratory, including a sample dating to 1450–1220 BC from Tell Medinet Ghurabm, a town in the Fayoum area of Egypt that was excavated between 1888 and 1890 by Sir Flinders Petrie (data now shown). Degradation is a significant problem for identification, but exposure of a fresh surface may help in collecting a good quality spectrum.

FT-Raman spectroscopy may also prove useful in phytochemical studies. Interest in natural products such as resins is increasing, particularly their medicinal properties. FT-Raman spectroscopy can provide information on the components within the resin and how these components are affected by factors such as oxidation and hydrolysis. Furthermore, identification of common components within resins has implications on the biodiversity and taxonomic variation within and between geographic regions.

REFERENCES

1. Fox, A.; Heron, C.; Sutton, M. Q. Archaeometry 1995, 37, 363–375.
2. Mills, J. S.; White, R. Stud Conserv 1997, 22, 12–31.
3. Fraquet, H. Amber; Butterworths: London, 1987.
4. Howes, F. N. Vegetable Gums and Resins; Chronica Botanica Company: Waltham, MA, 1949.
5. Mahajan, B.; Taneja, S. C.; Sethi, V. K.; Dhar, K. L. Phytochemistry 1995, 39, 453–455.
6. Edwards, H. G. M.; Farwell, D. W.; Daffner, L. Spectrochim Acta Part A 1996, 52, 1639–1648.
7. Edwards, H. G. M.; Falk, M. J. J Raman Spectrosc 1997, 28, 211–218.
8. Edwards, H. G. M.; Falk, M. J. Spectrochim Acta Part A 1997, 53, 2393–2401.
9. Edwards, H. G. M.; Sibley, M. G.; Heron, C. Spectrochim Acta Part A 1997, 53, 2373–2382.
10. Edwards, H. G. M.; Farwell, D. W.; Quye, A. J Raman Spectrosc 1997, 28, 243–249.
11. Edwards, H. G. M.; Falk, M. J.; Sibley, M. G.; Alvarez-Benedi, J.; Rull, F. Spectrochim Acta Part A 1998, 54, 903–920.
12. Stern, B., personal communication, 2000.
13. Wiendl, R. M.; Muller, B. M.; Franz, G. Carbohydr Polym 1995, 28, 217– 226.